Tissue variation in the control of oxidative phosphorylation: implication for mitochondrial diseases

Rodrigue ROSSIGNOL, Thierry LETELLIER[1], Monique MALGAT, Christophe ROCHER and Jean-Pierre MAZAT
INSERM EMI 99-29, Université Victor Segalen-Bordeaux 2, 146 rue Léo-Saignat, F-33076 Bordeaux-cedex, France

Metabolic control analysis has often been used for quantitative studies of the regulation of mitochondrial oxidative phosphorylations (OXPHOS). The main contribution of this work has been to show that the control of mitochondrial metabolic fluxes can be shared among several steps of the oxidative phosphorylation process, and that this distribution can vary according to the steady state and the tissue. However, these studies do not show whether this observed variation in the OXPHOS control is due to the experimental conditions or to the nature of the mitochondria. To find out if there actually exists a tissue variation in the distribution of OXPHOS control coefficients, we determined the control coefficients of seven OXPHOS complexes on the oxygen-consumption flux in rat mitochondria isolated from five different tissues under identical experimental conditions. Thus in this work, only the nature of the mitochondria can be responsible for any variation detected in the control coefficient values between different tissues. The analysis of control coefficient distribution shows two tissue groups: (i) the muscle and the heart, controlled essentially at the level of the respiratory chain; and (ii) the liver, the kidney and the brain, controlled mainly at the phosphorylation level by ATP synthase and the phosphate carrier. We propose that this variation in control coefficient according to the tissue origin of the mitochondria can explain part of the tissue specificity observed in mitochondrial cytopathies.

Key words: metabolic control analysis, mitochondria, tissue specificity.

INTRODUCTION

Metabolic control analysis [1–3] has often been used for quantitative studies of the regulation of mitochondrial oxidative phosphorylations (OXPHOS) [4–25]. The main contribution of this work has been to show that the control of mitochondrial metabolic fluxes (oxygen consumption and ATP synthesis) can be shared among several steps of the oxidative phosphorylation process, and that this distribution can vary according to the steady state and the tissue. However, these studies do not allow us to conclude whether this observed variation is due to the nature of the mitochondria or to the experimental conditions. Indeed, many parameters, such as temperature, pH, buffer composition and respiratory substrate, can change the respiratory steady state and therefore modify the control coefficient distribution.

In this work, to ensure that the observed control coefficient variations can only be attributed to the properties of the tissue's mitochondria, we have chosen to study mitochondria isolated from different tissues under the same experimental conditions. In this way, we have determined the control coefficients of seven OXPHOS complexes [complex I, complex III, complex IV, ATP synthase, adenine nucleotide translocator (ANT), phosphate carrier and pyruvate carrier] on the oxygen-consumption flux in rat mitochondria isolated from five different tissues (muscle, heart, liver, kidney and brain).

The present results show clearly that under our conditions, tissue variation exists in the distribution of OXPHOS control. In addition, whatever the tissue origin of the mitochondria, this control is distributed largely between the different OXPHOS enzymic complexes, indicating that there is no limiting step, as can be predicted from the metabolic control theory [26,27].

The analysis of control-coefficient distribution shows two tissue groups: (i) the muscle and the heart, controlled essentially at the level of the respiratory chain; and (ii) the liver, the kidney and the brain, controlled mainly at the phosphorylation level by ATP synthase and the phosphate carrier. It also appears that the quantity of enzymic complexes can be one of the possible parameters that intervene in the tissue variation of the OXPHOS control. This is illustrated by the comparative study of the ANT control in liver and in muscle.

Finally, we discuss our results in the context of mitochondrial cytopathies [28–33] in which a tissue specificity has been observed: it is characterized by the fact that even if a defect in a given OXPHOS complex is present in all tissues, only some will be affected [31,34–37]. We propose that the variation in control coefficient values for such a complex according to the tissue origin of the mitochondria can partly explain the tissue specificity observed in mitochondrial diseases.

MATERIALS AND METHODS

Chemicals

Antimycin, carboxyatractyloside (CATR), KCN, α-cyano-4-hydroxycinnamate (C4H), oligomycin, rotenone and *N*,*N*,*N*′,*N*′-tetramethyl-*p*-phenylenediamine (TMPD) were from Sigma.

Animals

Male Wistar rats weighing 200–300 g having free access to water and standard laboratory diet were used for this study. After 1 day of starvation, animals were killed by cervical shock and decapitation.

Preparation of rat muscle and heart mitochondria

To have enough muscle mass to obtain sufficient mitochondrial protein, the hind-limb muscles were used, i.e. the gastrocnemius

Abbreviations used: OXPHOS, mitochondrial oxidative phosphorylations; ANT, adenine nucleotide translocator; CATR, carboxyatractyloside; TMPD, *N*,*N*,*N*′,*N*′-tetramethyl-*p*-phenylenediamine; C4H, α-cyano-4-hydroxycinnamate.

[1] To whom correspondence should be addressed (e-mail tletel@u-bordeaux2.fr).

(G), the plantaris (P) and the soleus (S). Rapidly removed from the bones, the muscles were immersed in high-EDTA buffer and freed from tendons and paratendinous tissue, visible fat and connective tissue. Rat muscle mitochondria were isolated by differential centrifugation as described by Morgan-Hughes et al. [38]. Muscle of the two hindlegs was collected in isolation medium I (210 mM mannitol, 70 mM sucrose, 50 mM Tris/HCl, pH 7.4 and 10 mM EDTA) and digested by trypsin (0.5 mg/g of muscle) for 30 min. The reaction was stopped by addition of trypsin inhibitor (soya bean inhibitor to trypsin, 3:1). The homogenate was centrifuged at 1000 ***g*** for 5 min. The supernatant was strained on gauze and recentrifuged at 7000 ***g*** for 10 min. The resulting pellet was resuspended in ice-cold isolation medium II (225 mM mannitol, 75 mM sucrose, 10 mM Tris/HCl, pH 7.4, and 0.1 mM EDTA) and a new series of centrifugations (1000 and 7000 ***g***) was performed. The last mitochondrial pellet was resuspended in a minimum volume of isolation medium II to obtain a mitochondrial concentration of between 50 and 80 mg/ml. Protein concentration was estimated by the Biuret method [39] using BSA as standard. Heart mitochondria were isolated according to the same procedure as for muscle mitochondria, and to obtain a sufficient mitochondrial protein content two rat hearts were used.

Preparation of rat liver and kidney mitochondria

Liver mitochondria were isolated by differential centrifugation as described by Johnson and Lardy [40], with some modifications. Liver was collected in isolation medium A (250 mM sucrose, 10 mM Tris/HCl, pH 7.6, and 1 mM EGTA) and homogenized. The homogenate was centrifuged at 1000 ***g*** for 5 min. The supernatant was strained on gauze and recentrifuged at 7000 ***g*** for 10 min. The resulting pellet was resuspended in ice-cold isolation medium B (250 mM sucrose, 10 mM Tris/HCl, pH 7.6, and 0.1 mM EGTA) and a new series of centrifugations (1000 and 7000 ***g***) was performed. The last mitochondrial pellet was resuspended in a minimum volume of isolation medium B to obtain a mitochondrial concentration of between 50 and 70 mg/ml.

Kidney mitochondria were prepared according to the same method [40]. Four kidneys were homogenized (after first removing the capsule). The homogenate was then treated in the same way as the liver preparation. The isolation media were the same as those used for the liver, and the last mitochondrial pellet was resuspended in a minimum volume of isolation medium B to obtain a mitochondrial concentration of between 40 and 60 mg/ml.

Preparation of rat brain mitochondria

Brain mitochondria were isolated from whole brain according to the method described by Clark and Nicklas [41]. Rats were killed by decapitation without stunning and the brains (seven brains at a time) were removed into isolation buffer (250 mM sucrose, 10 mM Tris/HCl, pH 7.4, and 0.5 mM K^+EDTA) and homogenized. The homogenate was centrifuged at 1000 ***g*** for 5 min. The supernatant was strained on gauze and recentrifuged at 7000 ***g*** for 10 min. The resulting pellet was resuspended in the same isolation buffer (ice-cold) and a new series of centrifugations (1000 and 7000 ***g***) was performed.

The crude mitochondrial pellet was resuspended in a final volume of 10 ml in 3% Ficoll medium (3% Ficoll, 250 mM sucrose, 10 mM Tris/HCl, pH 7.4, and 0.5 mM K^+EDTA). This suspension was layered carefully on to 20 ml of 6% Ficoll medium (6% Ficoll, 250 mM sucrose, 10 mM Tris/HCl, pH 7.4, and 0.5 mM K^+EDTA) and centrifuged for 30 min at 11500 ***g***. The mitochondrial pellet was resuspended in isolation medium and recentrifuged for 10 min at 12500 ***g***. The mitochondria were made up to a concentration of 60–70 mg of protein/ml in the isolation buffer.

Polarographic measurements

Mitochondrial oxygen consumption was monitored at 30 °C in a 1-ml thermostatically controlled chamber equipped with a Clarke oxygen electrode, in the following respiration buffer: 75 mM mannitol, 25 mM sucrose, 100 mM KCl, 10 mM Tris/phosphate, 10 mM Tris/HCl, pH 7.4, 50 μM EDTA plus respiratory substrate (10 mM pyruvate in the presence of 10 mM malate or 25 mM succinate). The mitochondrial concentration used for this study was 1 mg/ml and state 3 (according to Chance and Williams [42]) was obtained by addition of 2 mM ADP. The state 3 respiratory rates were expressed in nanoatoms of O/min per mg of protein and corresponded to the 100% respiratory rates of Figures 1–7 (see below). These values measured on mitochondria isolated from different tissues show that one can consider the mitochondria to have been in the same steady state of respiration, whatever their tissue origin (muscle, 170 ± 36; heart, 189 ± 41; liver, 142 ± 21; kidney, 165 ± 21 nanoatoms of O/min per mg of protein), with the exception of the brain, where the state 3 respiratory rate presents an inferior value (128 ± 32 nanoatoms of O/min per mg of protein).

The respiratory control ratio is defined as the ratio of state 3 (in the presence of ADP) to state 4 (in the absence of ADP) respiratory rates. The values we obtained on mitochondria isolated from the different tissues were, for muscle, 4.5 ± 2.1; for heart, 5.1 ± 1.2; for liver, 3.2 ± 1.1; for kidney, 4.4 ± 1.9; and for brain, 2.6 ± 1.4. All these values (state 3 and respiratory control ratios) represent the means $\pm$ S.E.M. of at least nine different mitochondria isolations.

Enzymic determination

Complex I (NADH ubiquinone reductase)

The oxidation of NADH by complex I was recorded using the ubiquinone analogue decylubiquinone as electron acceptor [43]. The basic assay medium (35 mM KH_2PO_4, 5 mM $MgCl_2$ and 2 mM KCN, pH 7.2) was supplemented with defatted BSA (2.5 mg/ml), antimycin A (5 μg/ml), 65 μM decylubiquinone and 0.13 mM NADH in a final volume of 1 ml. The enzyme activity was measured by starting the reaction with 50 μg of mitochondrial protein. The decrease in absorption due to NADH oxidation was measured at 340 nm both in the absence and in the presence of 5 μg/ml rotenone. The difference, ΔI, in activities gives the rotenone-sensitive activity of complex I.

Complex III (ubiquinol cytochrome *c* reductase)

The oxidation of 20 μM decylubiquinone by complex III was determined using cytochrome *c* (III) as electron acceptor [43]. The assay was carried out in basic medium supplemented with 2.5 mg/ml defatted BSA, 15 μM cytochrome *c* (III) and 5 μg/ml rotenone. The reaction was started with 10 μg of mitochondrial protein and the enzyme activity was measured at 550 nm.

Complex IV (cytochrome *c* oxidase)

Two methods for the determination of cytochrome *c* oxidase activity were used. In the first one, cytochrome *c* oxidase activity was determined spectrophotometrically [44] using cytochrome *c* (II) as substrate. The oxidation of cytochrome *c* was monitored at 550 nm at 30 °C. In the second method, we isolated cytochrome

c oxidase activity from the rest of the respiratory chain with rotenone, antimycin, and using 3 mM ascorbate and 0.5 mM TMPD as an electron-donor system. The respiratory rate was then monitored according to the polarographic method described above.

Control coefficient determination

The control coefficients of various steps involved in the oxidative phosphorylations were determined using the inhibitor method [8]. This method is based on determination of the global-flux (oxygen consumption or respiratory rate) and the isolated-step (OXPHOS complex) activity titration curves, performed with specific inhibitors. In this case the control coefficient of step i on flux J is calculated by:

$$C_i^J = \frac{\partial \ln J}{\partial \mathrm{I}} \Big/ \frac{\partial \ln v_i}{\partial \mathrm{I}} | \text{steady state I} = 0$$

where the control coefficient, C, is equal to the ratio of the initial slope of the inhibition curve of the global flux J over the initial slope of the inhibition curve of the isolated-step activity v_i, determined in the same conditions as for the global flux.

The global flux J studied was the mitochondrial oxygen consumption flux followed by polarography at state 3 by using 10 mM pyruvate and 10 mM malate as substrates in the presence of 2 mM ADP. The specific inhibitors used were: rotenone for complex I, antimycin for complex III, KCN for complex IV, oligomycin for ATP synthase, CATR for ANT, mersalyl for the phosphate carrier and C4H for the pyruvate carrier.

For complexes I, III and IV, the inhibition curves of the activities of enzymic complexes (isolated-step activities) were determined experimentally. However, in some cases, it was impossible to determine the activity of the isolated step in the same conditions as for the global flux. This was the case for ATP synthase, ANT, the phosphate carrier and the pyruvate carrier, the activities of which are dependent on the amount of $\Delta\mu_{H^+}$ generated by the respiratory chain. In these cases, the method presented by Gellerich et al. [7] was used. This mathematical model was designed to estimate flux control coefficients from titration studies with specific non-competitive inhibitors. Indeed, it is considered that (i) the inhibitor binds specifically to the enzyme that is in the metabolic network and (ii) assuming non-competitive inhibition, the binding is independent of the concentration of the metabolic intermediates. The general interest of this model is that, in contrast with the graphical determination of the initial slope based on the first points of each titration curve, it pays attention to the whole set of data. This method uses a non-linear regression that fits the respiratory rate inhibition curve with the model. Non-linear fitting was done using the program Simfit [45]. From the parameters obtained by this fitting procedure and the model equations, we drew the inhibition curve of the isolated-step activity with the program TK Solver Plus (Universal Technical Systems, Rockford, IL, U.S.A.). The flux control coefficient values of the various steps involved in the oxidative phosphorylations were also calculated using this model.

For complexes I, III and IV, a second method was also used to calculate the control coefficients. Indeed, in those cases where the inhibition curve of the isolated-step activity could be determined experimentally, we used a graphical method based on the initial-slope determinations by a linear regression on the first points of both the global-flux and the isolated-step inhibition curves.

RESULTS

Oxygen consumption flux control coefficients for various OXPHOS steps in different tissues

For each control coefficient determination, we used the same respiratory buffer and the same experimental conditions. Under these conditions, the different respiratory rates (states 4 and 3 according to Chance and Williams [42]) and the respiratory control ratios were determined (see the Materials and methods section).

Complex I control coefficients

Titration curves of the respiratory rate (global flux) are presented for the five tissues in Figure 1. The model of Gellerich et al. [7] does not allow the adjustment of those inhibition curves, and so the determination of control coefficients has necessitated experimental determination of the isolated-step activity inhibition (Figure 1). Moreover, in the case of the kidney, although the titration curve of the global flux could be fitted by the model, the inhibition curve of the isolated-step activity drawn by this

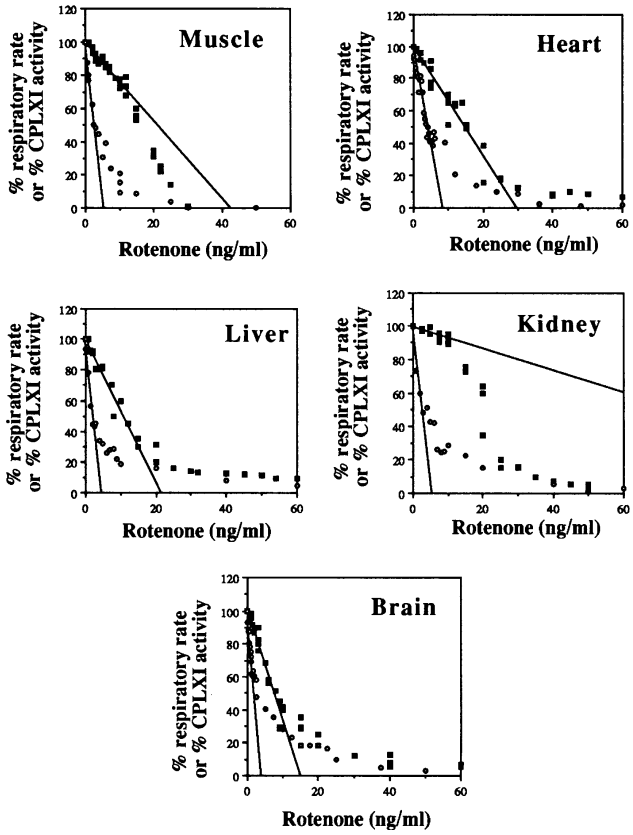

Figure 1 Complex (CPLX) I titration curves

Percentage of oxygen consumption flux (■) and percentage of isolated-step activity (○) as a function of rotenone concentration in rat mitochondria isolated from muscle, heart, liver, kidney and brain. Inhibition of oxygen consumption flux was followed by polarography at state 3 by using 10 mM pyruvate and 10 mM malate as substrates in the presence of 2 mM ADP. The control (100%) oxygen consumption rates are listed in the Materials and methods section. Isolated-step activity was recorded spectrophotometrically as described in the Materials and methods section.

Table 1 Control coefficient values of different OXPHOS complexes in mitochondria isolated from different tissues

Control coefficient values were determined according to the graphic method for complexes I and III whereas the fitting procedure was used for all the other complexes. Data represent the mean ± S.E.M. obtained with five different mitochondrial preparations.

	Control coefficient				
	Muscle	Heart	Liver	Kidney	Brain
Complex I	0.13 ± 0.03	0.26 ± 0.04	0.27 ± 0.03	0.06 ± 0.05	0.25 ± 0.05
Complex III	0.22 ± 0.05	0.19 ± 0.01	0.07 ± 0.03	0.02 ± 0.06	0.02 ± 0.02
Complex IV	0.2 ± 0.04	0.13 ± 0.01	0.03 ± 0.02	0.04 ± 0.02	0.02 ± 0.01
ATP synthase	0.1 ± 0.04	0.12 ± 0.02	0.2 ± 0.03	0.27 ± 0.08	0.26 ± 0.05
ANT	0.08 ± 0.03	0.04 ± 0.02	0.01 ± 0.02	0.07 ± 0.02	0.08 ± 0.03
Phosphate carrier	0.08 ± 0.03	0.14 ± 0.04	0.26 ± 0.05	0.28 ± 0.09	0.26 ± 0.05
Pyruvate carrier	0.2 ± 0.08	0.15 ± 0.03	0.21 ± 0.06	0.03 ± 0.02	0.26 ± 0.06
Σ	1.02 ± 0.16	1.05 ± 0.08	1.06 ± 0.15	0.81 ± 0.22	1.16 ± 0.13

model did not correspond to the experimental curve. This difference can be explained by the discrepancy between the model and the type of inhibitor used [13]; indeed, the model considers pure non-competitive inhibition, which is not the case for rotenone.

In Figure 1, experimental isolated-step activity inhibition curves present similar shapes in the different tissues. Moreover, the regression line performed on the first points of these curves cuts the *x* axis at a value of approx. 5 ng of rotenone/mg of protein.

Control coefficient values calculated by the graphic method are given in Table 1. In our study and except for the kidney, complex I appears to be a major controlling step on oxygen consumption flux, whatever the tissue origin of the mitochondria. Indeed, the complex I control coefficient values (0.13–0.27) were comparable with those obtained by Doussière et al. [5] and Moreno-Sanchez et al. [18] on rat heart mitochondria (0.37 and 0.13), but also by Davey and Clark [46] on rat brain mitochondria (0.14) and by Letellier et al. [13] and Korzeniewski and Mazat [11] on muscle mitochondria (0.11–0.12). The lower value we obtained in the kidney (0.06) has also been found by Moreno-Sanchez et al. [18].

On the other hand, it was not possible to compare control-coefficient values obtained in liver mitochondria with those of the literature. Indeed, although this tissue has been studied by many authors, the complex I control coefficient was not determined because the respiratory substrate used in these studies was succinate [7,8,10,12,17,20,23,24].

Complex III control coefficients

As for complex I, control coefficient calculation required the experimental determination of the isolated-step activity inhibition curve. In Figure 2, the isolated-step activity inhibition curves present a similar shape whatever the tissue origin of the mitochondria, and the regression lines based on the first points of the curves cut the *x* axes at values of around 7 ng of antimycin/mg of protein.

Complex III control coefficients on the oxygen consumption flux calculated by the graphic method are given in Table 1. The complex III control coefficient distribution shows two types of tissue. Indeed, complex III shows more control in muscle (0.22) and heart (0.19) than in liver (0.07), kidney (0.02) and brain (0.02).These values are comparable with those found in muscle mitochondria by Gellerich et al. [7] and Letellier et al. [13] (0.17 and 0.13), but also in heart mitochondria by Moreno-Sanchez et al. [18] (0.11).

Studies performed on liver mitochondria [7,8,10,20,24] give values for the complex III control coefficient of between 0.03 and 0.3. With succinate being used as a respiratory substrate in these

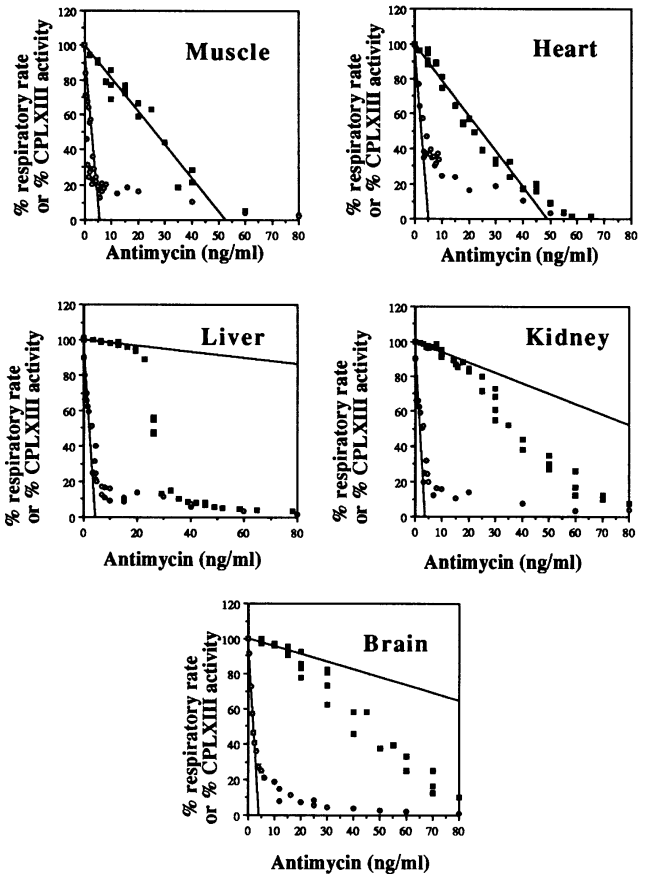

Figure 2 Complex (CPLX) III titration curves

Percentage of oxygen consumption flux (■) and percentage of isolated-step activity (○) as a function of antimycin concentration in rat mitochondria isolated from muscle, heart, liver, kidney and brain. Details are as for Figure 1.

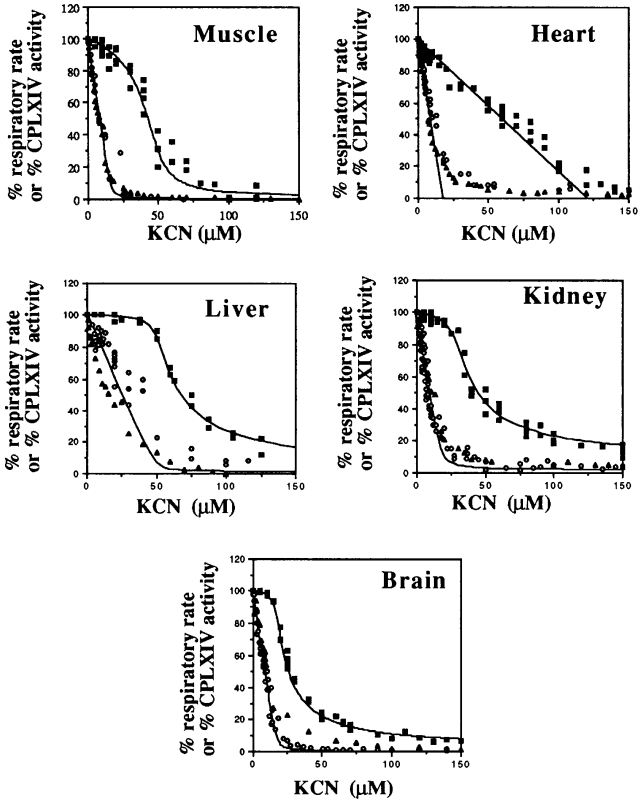

Figure 3 Complex (CPLX) IV titration curves

Percentage of oxygen consumption flux (■) and percentage of isolated-step activity as a function of KCN concentration in rat mitochondria isolated from muscle, heart, liver, kidney and brain. Inhibition of oxygen consumption flux was followed by polarography at state 3 by using 10 mM pyruvate and 10 mM malate as substrates in the presence of 2 mM ADP. The control (100%) oxygen consumption rates are listed in the Materials and methods section. Isolated-step activity was plotted (i) by following spectrophotometrically the oxidation of cytochrome *c* at 550 nm (○), (ii) by polarography with 3 mM ascorbate and 0.5 mM TMPD as an electron-donor system (▲) or (iii) by the program Simfit [45], using the parameters obtained by the fitting procedure (lines) [7].

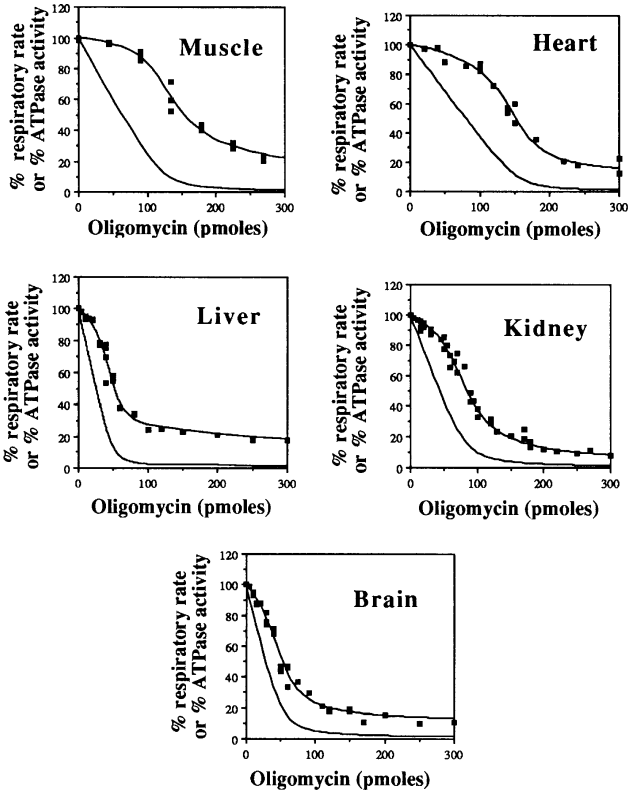

Figure 4 ATP synthase titration curves

Percentage of oxygen consumption flux and percentage of isolated-step activity as a function of oligomycin concentration in rat mitochondria isolated from muscle, heart, liver, kidney and brain. The inhibition of oxygen consumption flux (■) was followed as for Figure 1. The line passing through the squares corresponds to the fitting of the experimental data to the model of Gellerich et al. [7]. Isolated-step activity inhibition curve (line without points) was drawn using the Simfit program [45].

studies, it has been impossible to make a comparison with our results. On the other hand, the control coefficient that we have obtained in brain (0.02) is in contradiction with the value reported by Davey and Clark [46] (0.15). This may be explained by the use of a different respiratory buffer.

Complex IV control coefficients

For cytochrome *c* oxidase, the determinations of the isolated-step activity inhibition curves were obtained by (i) polarography, (ii) spectrophotometry and (iii) using the parameters obtained by the fitting procedure. These three methods gave almost the same curves (Figure 3) and then the same control coefficient values.

Complex IV control coefficients on the oxygen consumption flux determined by the fitting procedure are given in Table 1. As for complex III and according to the control coefficient values, two types of tissues can be distinguished. Indeed, complex IV shows more control in muscle (0.20) and heart (0.13) than in liver (0.03), kidney (0.04) or brain (0.02). These values are comparable with those obtained from muscle mitochondria by Moreno-Sanchez [17] (0.12) and Letellier et al. [13] (0.12 and 0.17). For the liver, when succinate is used as a respiratory substrate, values found in the literature give a control coefficient of around 0.2 [8,12,20,24]. On the other hand, in our study, where pyruvate was used as a respiratory substrate, the complex IV control coefficient value was lower (0.03). This result with pyruvate was also obtained by Moreno-Sanchez [17].

For the kidney, complex IV control coefficient values are in agreement with those found by Moreno-Sanchez [17], whereas for the brain, Davey et al. [46,47] obtained a higher control for this step (0.13–0.24). As for complex III, this discrepancy may be explained by the use of a different respiratory buffer or different respiratory substrate. Indeed, Davey et al. used glutamate in the presence of malate as respiratory substrate instead of pyruvate/malate in our study. In addition, we have used a whole-brain preparation instead of synaptosomal [47] or non-synaptic [46] mitochondria. Furthermore, these authors have already emphasized different complex I and IV control coefficients for these two types of brain mitochondria [48].

ATP synthase control coefficients

With the inhibition of the isolated-step activity being inaccessible experimentally, we have considered that oligomycin behaves according to a non-competitive quasi-irreversible model [12]. We then employed the fitting method to determine the control coefficient of the ATPase on the oxygen-consumption flux (Figure 4). The values obtained are given in Table 1. Again, ATPase control coefficients on the oxygen consumption flux show two

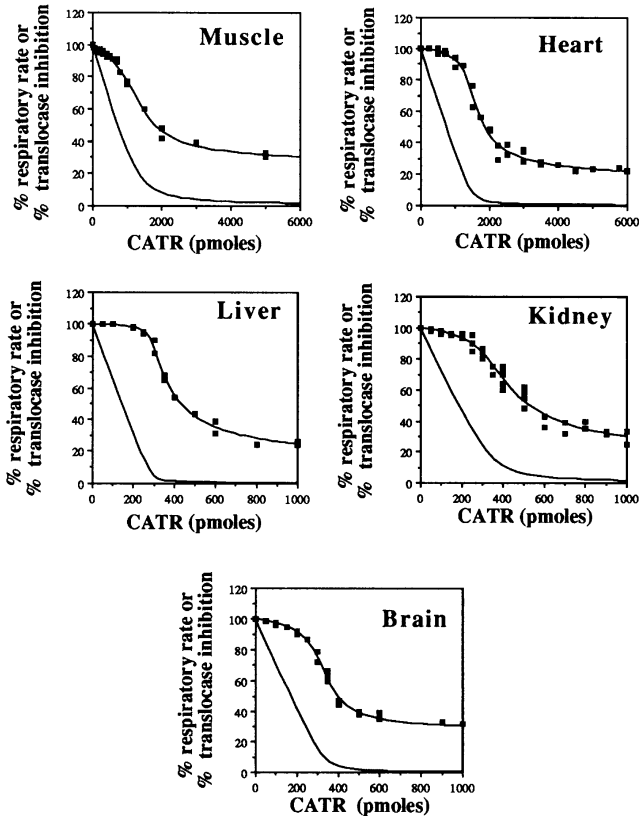

Figure 5 ANT titration curves

Percentage of oxygen consumption flux and percentage of isolated-step activity as a function of CATR concentration in rat mitochondria isolated from muscle, heart, liver, kidney and brain. Details are as for Figure 4.

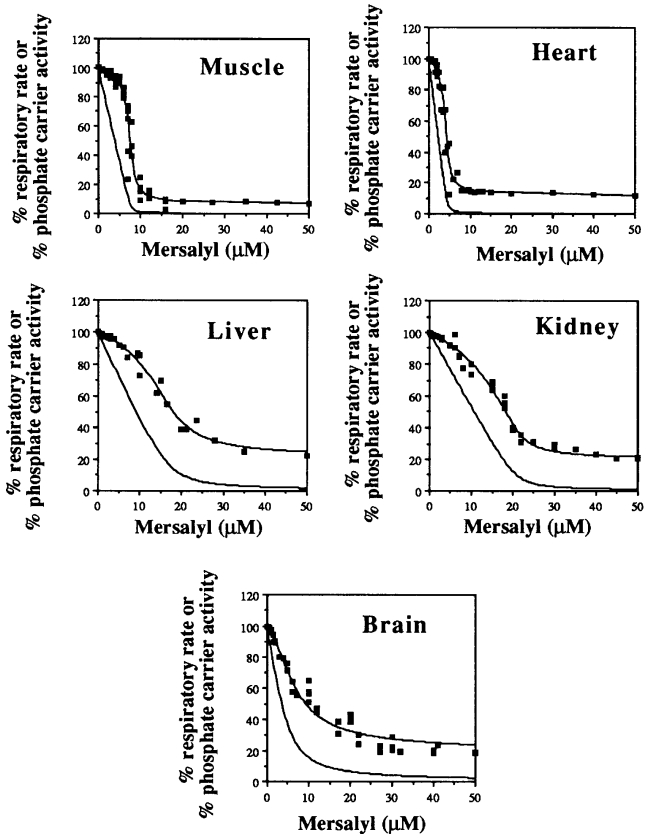

Figure 6 Phosphate carrier titration curves

Percentage of oxygen consumption flux and percentage of isolated-step activity as a function of mersalyl concentration in rat mitochondria isolated from muscle, heart, liver, kidney and brain. Details are as for Figure 4.

groups of tissues, but in contrast with complexes III and IV, in liver, kidney and brain, ATPase exerts a stronger control (0.20, 0.27 and 0.26, respectively) than in muscle and heart (0.10 and 0.12, respectively). These values are comparable with those found by many authors [7,8,22,24].

ANT control coefficients

As for oligomycin, we have considered that CATR behaves according to an irreversible non-competitive model [12]. We then employed the fitting method to determine the control coefficient of the ANT on the oxygen consumption flux (Figure 5). The values obtained are given in Table 1.

Under our experimental conditions and whatever the tissue origin of the mitochondria, the ANT appears to be a very minor controlling step of the oxygen-consumption flux. However, for rat liver mitochondria, it was surprising to find very minor control by the ANT (0.01). Indeed, many authors [10,20,24] give this step as a major controlling one, with a control coefficient varying between 0.17 and 0.32 when succinate is used as a respiratory substrate. Therefore, the nature of the respiratory substrate seems to play an important role in the control coefficient value. To verify this hypothesis, we determined the ANT control coefficients under our experimental conditions but with succinate as a respiratory substrate. In those conditions (results not shown), the value obtained for the liver (0.23 ± 0.04) was comparable with those of the literature [10,20,24], whereas for muscle this change of respiratory substrate leads to no variation in the control coefficient value (0.05 ± 0.02).

Phosphate-carrier control coefficients

Control coefficient values given by fitting the titration curves (Figure 6) are summarized in Table 1. Results obtained for the phosphate carrier again show two groups of tissues. Indeed, in muscle and heart, the phosphate carrier exerts lower control (0.08 and 0.14) than in liver, kidney and brain (0.26, 0.28 and 0.26).

Pyruvate carrier control coefficients

Control-coefficient values given by the fitting procedure are summarized in Table 1. The pyruvate carrier exerts a rather important control (around 0.2) on the oxygen consumption flux whatever the tissue origin of the mitochondria, except for the kidney (0.03). This low control value for the kidney can be linked to the amount of C4H giving maximal inhibition of the flux (around 200 nmol of C4H/mg of protein), which is 100 times higher in kidney than in other tissues (Figure 7). This observation is in good agreement with the work of Halestrap and Denton

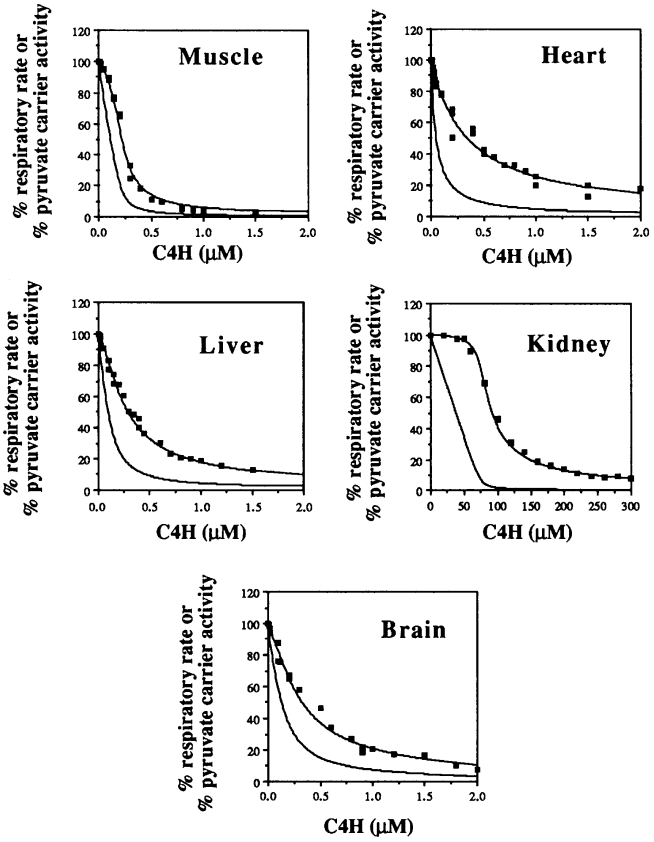

Figure 7 Pyruvate carrier titration curves

Percentage of oxygen consumption flux and percentage of isolated-step activity as a function of C4H concentration in rat mitochondria isolated from muscle, heart, liver, kidney and brain. Details are as for Figure 4.

Table 2 Amount of inhibitor (*I*) of ATP synthase (oligomycin) and ANT (CATR) giving maximal inhibition of respiratory flux

The data, expressed in pmol/mg of protein, represent the means ± S.E.M. obtained with five different mitochondrial preparations.

	Amount of inhibitor				
	Muscle	Heart	Liver	Kidney	Brain
ATP synthase	217 ± 33	200 ± 25	66 ± 24	103 ± 18	70 ± 17
ANT	1786 ± 258	1425 ± 381	517 ± 147	499 ± 149	380 ± 67

[49], who showed that 200 nmol of C4H/mg of protein was needed to inhibit the respiration in rat kidney mitochondria completely.

Enzymic complex quantification

Under our conditions, one of the intervening factors in the establishment of the respiratory steady state (and therefore in the distribution of control coefficients in the different tissues) can be a difference in the enzyme activity of the complexes. This difference of enzyme activity can be due to different quantities of enzyme (content of protein) or to different kinetic properties (different apparent K_m for instance) of the enzyme complexes.

We have studied the role of the quantity of enzymic complexes in each type of mitochondria on control coefficient distribution. Indeed, in the case of irreversible specific inhibitors, such as CATR and oligomycin [7,10], the amount of ATPase and ANT can be evaluated by the amount of inhibitor that gives the maximal inhibition of the global respiratory flux (Figures 4 and 5). Indeed, due to the strong affinity constants of these inhibitors, we can consider that the quantity of enzyme–inhibitor complex is directly proportional to the quantity of inhibitor added.

The quantification of ANT and ATP synthase (Table 2) allows us to distinguish two types of tissue: muscle and heart, 1.4–1.8 nmol of equivalent ANT and 0.2 nmol of equivalent ATPase per mg of protein; and liver, kidney and brain; 0.4–0.5 nmol of equivalent ANT and 0.07–0.1 nmol of equivalent ATPase per mg of protein.

DISCUSSION

Control of experimental conditions

According to the metabolic control theory, many parameters, the nature of mitochondria or the conditions of respiratory rate measurement (temperature, pH, buffer composition), can change the respiratory steady state and therefore modify the control-coefficient distribution. In this study, in order that observed control coefficient values could only be attributed to mitochondrial properties and not to variation in experimental conditions, it was important to control these conditions, for the mitochondria isolation as well as for the respiratory rate measurement. Thus in this study only the nature of the mitochondria can be responsible for a variation in control coefficient values between different tissues.

There is a significant risk of damaging mitochondria during their isolation and thus of modifying the control coefficient values. Indeed, a loss of cytochrome *c* or an increase of the leak may lead to a new steady state and therefore to a possible modification of control coefficient distribution. For this reason, we have chosen mitochondria isolation methods according to the authors' experience in this domain, their compatibility with the purpose of our study (that necessitates preservation of mitochondrial integrity) and their utilization frequency by other authors. A useful parameter to evaluate mitochondrial damage during isolation is the respiratory control ratio [42]. Therefore, in our study, we have used mitochondrial preparations only when the respiratory control ratio was close to values reported for the same tissues and under the same conditions (see the Materials and methods section).

In addition, we determined the choice of respiratory conditions to make sure that only the nature of the mitochondria could be responsible for the control coefficient distribution. Indeed, state 3 respiratory rate depends on experimental conditions and notably on the buffer composition. Because, in the literature, optimal respiratory buffers elaborated for mitochondria isolated from different tissues present too great a variation in their composition (phosphate concentration, isotonicity maintained by sucrose or KCl etc.) we used the same respiratory buffer for all titration experiments.

Finally, the experimental parameter that we chose to characterize the steady state of the oxidative phosphorylations was the state 3 respiratory rate value. These values measured in mitochondria isolated from different tissues show that one can consider the mitochondria in the same steady state of respiration, whatever their tissue origin (around 165 nanoatoms of O/min per mg of protein; see the Materials and methods section), with one exception for brain, where the state 3 respiratory rate

presents an inferior value (128 ± 32 nanoatoms O/min per mg of protein).

Titration curves and control coefficient determinations

To determine the control coefficients, we used the so-called inhibitor method [8]. When it was possible, we used the fitting procedure [7,45] to calculate the control coefficient. Notwithstanding the fact that it can be used when the isolated-step activity inhibition curve cannot be obtained experimentally, this procedure considers all points of the respiratory flux titration curve for the calculation. Another advantage of this method is that it allows us to draw the isolated-step activity inhibition curve from the parameters of the fit. One example of the use of this model is presented in Figure 3 where the experimental and fitted titration curves appear to be superimposable, which validates the fitting procedure.

However, if this method presents some advantages, the model is limited to non-competitive inhibitors and to global-flux titration curves of sigmoidal profile. This is the reason why it was impossible to fit the oxygen consumption titration curves performed with rotenone and antimycin. Nevertheless for these two inhibitors, even when the global-flux titration curve presented a sigmoidal shape, the isolated-step activity inhibition curves drawn from the parameters of the fit did not correspond to the experimental curves. These latter two cases illustrate the limitations of the model because the impossibility of fitting the experimental titration curves can be explained by the discrepancy between the model and the inhibitor used [13].

All the oxygen-consumption flux control coefficient values in different tissues are listed in Table 1. Whatever the tissue origin of the mitochondria, the sum of the control coefficients is approx. 1, as predicted by the metabolic control theory. However, the high standard deviations on the control coefficient totals (Table 1) illustrate the difficulty of either determining the isolated-step activity and the global-flux inhibition curves in the very same conditions or of calculating precisely the initial slopes of these curves in the graphical method. In addition, the lack of precision in the control coefficient value can also be due to the fitting model not corresponding exactly with the inhibitor used.

Control coefficients in different tissues

Under our experimental conditions and whatever the tissue origin of the mitochondria, the control was distributed largely between the different OXPHOS steps, indicating that there is no limiting step, as can be predicted from the metabolic control theory. Indeed, in this study, the control coefficient values were low and in the range of 0–0.28.

The pyruvate carrier is one of the most controlling steps in all the tissues (except for the kidney), indicating that even if the substrate delivery is not really embedded in the OXPHOS network, it plays under our conditions a rather important role in the oxygen consumption flux and it has to be taken into account for OXPHOS studies. On the other hand, the ANT has very low control coefficient values in all tissues, indicating that in our conditions the ADP supply is not a limiting step for mitochondrial respiration.

For the other complexes the analysis of control coefficient distribution shows two tissue groups: (i) muscle and heart controlled essentially at the level of the respiratory chain and (ii) liver, kidney and brain controlled mainly at the phosphorylation level by ATP synthase and the phosphate carrier.

All these observations show clearly that a tissue variation exists in the distribution of OXPHOS control and, with our experimental conditions, this variation can only be due to the nature of the mitochondria. However, *in vivo*, this phenomenon can also be due to different parameters, such as the cellular steady state, the energy demand and the energy supply of the tissue. For example in liver mitochondria, when the respiratory steady state is changed by using succinate as a respiratory substrate, the control coefficient of ANT becomes higher than when measured on pyruvate. In this case, in addition to the nature of mitochondria, the respiratory state of the tissue intervenes in the control coefficient distribution. Therefore, *in vivo*, the metabolic state of the tissue will play an important role in the distribution of the oxidative-phosphorylation control. Thus control coefficient distribution could change in the muscle between resting state and exercise, leading to changes in the controlling steps. This is illustrated in muscle by the regulatory role of the inorganic phosphate concentration in supply of the energy to the tissue [50]. Indeed, in this tissue, large variations in the phosphate concentration occur between resting state and exercise [51], and it has been shown that such changes modify the distribution of the OXPHOS control [15,17,24].

In addition, to point out the interest of the determination of control coefficients for the study of flux regulatory mechanisms, this work also shows that in the metabolic state the quantity of enzymic complex can be one of the parameters that intervenes in the tissue variation of the OXPHOS control. This can be illustrated by the study of ANT control in liver and muscle. Indeed, this step appears to exert low control in all the tissues (0.01–0.08) when the respiratory substrate is pyruvate. On the contrary, when the respiratory substrate is succinate, the control coefficient value of the translocator increases 20 times in liver, whereas it remains low in muscle. This phenomenon can be explained by the comparative analysis of the amount of translocator in liver and muscle. Indeed, we have shown that in liver the quantity of ANT is four times lower than in muscle (Table 2). Therefore, the quantity of translocator that was sufficient to support the respiratory flux (energy demand) during respiration on pyruvate (128.5 nanoatoms of O/min per mg) in both tissues became more limiting only in liver when the flux was increased by using succinate as a respiratory substrate (210 nanonatoms of O/min per mg). This limitation on succinate leads to a higher control coefficient of ANT in liver.

Control coefficients and tissue specificity of mitochondrial cytopathies

Mitochondrial pathologies are a heterogeneous group of metabolic disorders characterized by abnormalities of the mitochondrial ultrastructure as well as of oxidative phosphorylation functioning [28,30,31,52]. During the last few years, the study of mitochondrial DNA has shown, in a certain number of cases, some precise mutation sites associated with a better clinical definition of the related pathologies [32]. In addition, it has been shown that defects in oxidative phosphorylation are able to affect any tissue, thus leading to the concept of mitochondrial cytopathies [29]. Moreover, mitochondrial cytopathies present a tissue specificity characterized by the fact that even if a mutation is present in all tissues, only some will be affected, leading to the pathology [31,34–37]. Part of this phenomenon of tissue specificity can be explained by the variation of control coefficient values for a given complex according to the tissue origin of the mitochondria.

Indeed, we can assume that, for a given complex, the higher its control coefficient in a tissue, the more sensitive to a defect of that complex this tissue will be. For example, muscle and heart, which are controlled essentially at the level of the respiratory

chain, will be more sensitive to a respiratory-chain deficiency, whereas liver, kidney and brain would be more sensitive to a defect in phosphorylation. Therefore, in the case of a patient with the same cytochrome *c* oxidase deficiency in all tissues, the diminution of mitochondrial respiration would be more important in the heart than in the liver. In the same manner, mitochondrial respiration would be more affected by this deficiency in muscle compared with in the brain or the kidneys.

However, it is necessary to note that this study has been performed on rat mitochondria, under particular conditions that are far from the case *in vivo*. Indeed, we chose to work with experimental conditions where the variation of the control coefficient values could have only been due to the tissue nature of the mitochondria. For that reason, we chose experimental conditions imposing the same steady state of respiration. However, *in vivo*, tissues are in different steady states of respiration and one can think that this variation in steady state can play a role in the distribution of control coefficient values independently of the nature of the mitochondria. In this case, these two parameters (nature of the mitochondria and steady state of the tissue) could affect the distribution *in vivo* of the control coefficient in the tissue. Thus although our results cannot be extrapolated directly to mitochondrial cytopathies, they give evidence of the relevance of the control coefficient distribution in the phenomenon of tissue specificity.

We thank Dr. D. Fell and Dr. E. Gnaiger for stimulating discussions and Dr. R. Cooke and Ms. M.-N. Grangeon for correcting the English. This work was supported by the INSERM, the Association Française contre les Myopathies (A.F.M.), the Université Victor Ségalen Bordeaux 2 and the Région Aquitaine.

REFERENCES

1 Kacser, H. and Burns, J. A. in Rate Control of Biological Processes (1973) (Davies, D. D., ed.), pp. 65–104, Cambridge University Press, Cambridge
2 Heinrich, R. and Rapoport, T. A. (1974) Eur. J. Biochem. **42**, 89–95
3 Reder, C. (1988) J. Theor. Biol. **135**, 175–201
4 Brand, M., Hafner, R. and Brown, G. (1988) Biochem. J. **255**, 535–539
5 Doussière, J., Ligeti, E., Brandolin, G. and Vignais, P. V. (1984) Biochim. Biophys. Acta **766**, 492–500
6 Gellerich, F. N., Bohnensack, R. and Kunz, W. (1983) Biochim. Biophys. Acta **722**, 381–391
7 Gellerich, F. N., Kunz, W. S. and Bohnensack, R. (1990) FEBS Lett. **274**, 167–170
8 Groen, A. K., Wanders, R. J. A., Westerhoff, H. V., Van der Meer, R. and Tager, J. M. (1982) J. Biol. Chem. **257**, 2754–2757
9 Jouaville, L., Ichas, F., Letellier, T., Malgat, M. and Mazat, J. P. (1993) in Modern Trends in Biothermokinetics (Schuster, S., Rigoulet, M., Ouhabi, R. and Mazat, J. P., eds.), pp. 319–325, Plenum Press, New York
10 Jumelle-Laclau, M. (1993) Ph.D. Thesis, Université Victor Segalen–Bordeaux 2
11 Korzeniewski, B. and Mazat, J. (1996) Acta Biotheoret. **44**, 263–269
12 Kunz, W., Gellerich, F. N., Schild, L. and Schonfeld, P. (1988) FEBS Lett. **233**, 17–21
13 Letellier, T., Malgat, M. and Mazat, J. P. (1993) Biochim. Biophys. Acta **1141**, 58–64
14 Letellier, T., Malgat, M., Rossignol, R. and Mazat, J. P. (1998) Mol. Cell. Biochem. **148**, 409–417
15 Mazat, J. P., Jean-Bart, E., Rigoulet, M. and Guerin, B. (1986) Biochim. Biophys. Acta **849**, 7–15
16 Mazat, J. P., Letellier, T., Bédes, F., Malgat, M., Korzeniewski, B., Jouaville, L. S. and Morkuniene, R. (1997) Mol. Cell. Biochem. **174**, 143–148
17 Moreno-Sanchez, R. (1985) J. Biol. Chem. **260**, 12554–12560
18 Moreno-Sanchez, R., Devars, S., Lopez-Gomez, F., Uribe, A. and Corona, N. (1991) Biochim. Biophys. Acta **1060**, 284–292
19 Hafner, R., Brown, G. and Brand, M. (1989) Eur. J. Biochem. **188**, 313–319
20 Tager, J. M., Wanders, R. J. A., Groen, A. K., Kunz, W., Bohnensak, R., Kuster, U., Lekto, G., Boehme, G., Duszynski, J. and Wojtczak, L. (1983) FEBS Lett. **151**, 1–9
21 Taylor, R. W., Birch-Machin, M. A., Bartlett, K., Lowerson, S. A. and Turnbull, D. M. (1994) J. Biol. Chem. **269**, 3523–3528
22 Letellier, T., Heinrich, R., Malgat, M. and Mazat, J. P. (1994) Biochem. J. **302**, 171–174
23 Rolfe, D. F. S., Hulbert, A. J. and Brand, M. D. (1994) Biochim. Biophys. Acta **1118**, 405–416
24 Wisniewski, E., Kunz, W. S. and Gellerich, F. N. (1993) Eur. J. Biochem. **268**, 9343–9346
25 Wisniewski, E., Gellerich, F. N. and Kunz, W. S. (1995) Eur. J. Biochem. **230**, 549–554
26 Fell, D. (1992) Biochem. J. **286**, 313–330
27 Kacser, H. and Burns, J. A. (1980) Genetics **97**, 639–666
28 Di Mauro, S., Bonilla, E., Zeviani, M., Walton, J. and De Vivo, D. C. (1985) Ann. Neurol. **17**, 521–538
29 Di Mauro, S. and Moraes, C. (1993) Arch. Neurol. **50**, 1197–2008
30 Wallace, D. C. (1992) Annu. Rev. Biochem. **61**, 1175–1212
31 Wallace, D. C. (1993) Trends Genet. **9**, 128–133
32 Wallace, D. C., Lott, M. T., Brown, M. D., Huoponen, K. and Torroni, A. (1995) in Human Gene Mapping 1995: a Compendium (Cuticchia, A. J., ed.), pp. 910–954, Johns Hopkins University Press, Baltimore
33 Ballinger, S. W., Shoffner, J. M. and Wallace, D. C. (1994) Curr. Top. Bioenerg. **17**, 59–98
34 Chomyn, A. (1998) Am. J. Hum. Genet. **62**, 745–751
35 Schon, E. A., Bonilla, E. and DiMauro, S. (1997) J. Bioenerg. Biomembr. **29**, 131–149
36 Zhou, L., Chomyn, A., Attardi, G. and Miller, C. (1997) J. Neurosci. **17**, 7746–7753
37 Nonaka, I. (1992) Curr. Opin. Neurol. Neurosurg. **5**, 622–632
38 Morgan-Hughes, J. A., Darveniza, P., Kahn, S. N., Landon, D. N., Sherratt, R. M., Land, J. M. and Clark, J. B. (1977) Brain **100**, 617–640
39 Gornall, A. G., Bardawill, C. J. and David, M. M. (1949) J. Biol. Chem. **224**, 751–766
40 Johnson, D. and Lardy, H. (1967) Methods Enzymol. **10**, 94–96
41 Clark, J. B. and Nicklas, W. J. (1970) J. Biol. Chem. **245**, 4724–4731
42 Chance, B. and Williams, G. R. (1956) Adv. Enzymol. **17**, 65–134
43 Birch-Machin, M. A., Sheperd, M., Warmough, J., Sherratt, H. S. A., Bartlett, K., Darley-Usmar, V. M., Milligan, W. A., Welch, R. J., Aynsley-Green, A. and Turnbull, D. M. (1989) Pediatr. Res. **25**, 553–559
44 Wharton, D. C. and Tzagoloff, A. (1967) Methods Enzymol. **10**, 245–250
45 Holzhüter, H. G. and Colosimo, A. (1990) Comput. Appl. Biosci. **6**, 23–38
46 Davey, G. P. and Clark, J. B. (1996) J. Neurochem. **66**, 1617–1624
47 Davey, G. P., Penchen, S. and Clark, J. B. (1998) J. Biol. Chem. **273**, 12753–12757
48 Davey, G. P., Canavari, L. and Clark, J. B. (1997) J. Neurochem. **69**, 2564–2570
49 Halestrap, A. P. and Denton, R. M. (1975) Biochem. J. **148**, 97–106
50 From, A. H. L., Zimmer, S. D., Michurski, S. P., Mohanakrishnan, P., Ulstad, V. K., Thoma, W. J. and Ugurbil, K. (1990) Biochemistry **29**, 3731–3743
51 Kawano, Y., Tanokura, M. and Yamada, K. (1988) J. Physiol. (London) **407**, 243–261
52 Morgan-Hughes, J. A. (1986) in Myology (Engel, A. G. and Banker, B. Q., eds.), pp. 1709–1743, McGraw Hill, New York

Received 26 July 1999/25 October 1999; accepted 9 December 1999